AIAA SciTech Forum
4-8 January 2016, San Diego, California, USA
AIAA Infotech @ Aerospace

10.2514/6.2016-1982

Minimum Required Sensing Range for UAS Sense and Avoid Systems

Laith R. Sahawneh* , Jonathan Spencer † , Randal W. Beard ‡ and Karl F. Warnick §
Brigham Young University, Provo, Utah, 84602, USA

Development of effective sense and avoid systems is a critical challenge for operation of unmanned aircraft systems (UAS) in the National Airspace. A key issue is achieving detection of potential targets at sufficient range to achieve a low probability of collision with lightweight, low cost sensors suitable for UAS. We present a closed form analytical approach to designing the minimum required sensing range based on worst-case collision encounter geometries. Using a minimum safe distance of 500 ft and known velocities for several different aircraft, this minimum required sensing range is found to be approximately 1.861 km using slack parameter of $\delta_r = 0.0354$. We demonstrate that this is a feasible result by describing a radar sensor prototype that achieves the required minimum sensing range.

I. Introduction

The use of unmanned aircraft systems (UAS) in commercial and civil applications has been expanding rapidly in recent years. Many UAS missions will require simultaneous operation with existing airspace users. UAS currently face limitations on their access to the national airspace system (NAS) because they do not have the ability to sense and avoid other air traffic. Among many regulatory and technology issues, safety is the foremost concern and the most significant challenge before UAS integration into the NAS can be achieved. The Federal Aviation Adminstration (FAA), the national aviation authority in the United States, calls for an equivalent level of safety comparable to the see and avoid requirement for manned aircraft.

A robust, and reliable sense and avoid (SAA) system will be necessary for UAS to provide the required equivalent level of safety as manned aircraft. Typically, a complete functional sense and avoid system is comprised of sensors and associated trackers, collision detection, and collision avoidance. The main role of the sensor and tracker is to detect any of the various types of hazards, such as traffic or terrain, and track the motion of the detected object to gain sufficient confidence that the detection is valid. Electro-optical cameras, infrared, Light Detection And Ranging (LiDAR), and radar are examples of sensors to detect non-cooperative traffic.[1] Non-cooperative traffic means that data about conflicting traffic is not communicated or transmitted to the UAS from the conflicting intruders or from Air Traffic Control (ATC). Traffic and Collision Avoidance System (TCAS) and Automatic Dependent Surveillance-Broadcast (ADS-B) are examples of systems for detecting cooperative intruders.

Not every aircraft that is observed by the sensing system presents a risk of collision. Therefore the collision detection algorithm must determine whether or not an approaching intruder aircraft is on a collision course. The collision avoidance functionality involves the computation of a collision-free path while optimizing an objective function or performance metric. A collision avoidance maneuver is considered as the last resort effort to conceivably steer the UAS onto a safe course to prevent an imminent collision and may be achieved by means of an aggressive change in flight path.

The design of an SAA system for UAS should also address regulatory requirements, and performance and reliability standards. Initial efforts to address performance, design, construction, and reliability requirements of SAA system for UAS are all discussed in the TR F2411-07, standard document produced by ASTM international.[2] An excellent review of existing regulations, standards, recommended practices along with

*Research assistant, Department of Electrical and Computer Engineering, Brigham Young University.
†Research assistant, Department of Electrical and Computer Engineering, Brigham Young University.
‡Professor, Department of Electrical and Computer Engineering, Brigham Young University
§Professor, Department of Electrical and Computer Engineering, Brigham Young University

suggestions and recommendation for SAA requirements to facilitate the UAS integration into the NAS system are discussed in Ref. 3–5. Specific design parameters required by the SAA system such as sensor angular resolution, field of view, and minimum time, and sensing range needed to prevent a collision assuming a 2D head-on encounter geometry is addressed in Ref. 6. A radar-based sensor and tracking requirements are derived for a 2D flight head-on collision scenario combining worst-case scenarios and exhaustive Monte Carlo Simulations in Ref. 7. The authors in Ref. 8 propose a framework that consists of a target level of safety (TLS) approach using an event tree format to develop specific SAA effectiveness standards linking UAS characteristics and operating environments to midair collision risk quantified by a fatality rate.

Among these requirements and design specifications, developing a sensor that achieves a sufficiently large target detection range for effective collision avoidance is a crucial aspect of a viable SAA solution. Among many possible sensor modalities that can be used for UAS sense and avoid system, radar makes a reasonable choice for sense and avoid applications,[7,9,10] in particular to detect non-cooperative intruders. Recent progress in radar technology and advancement in integrated circuit fabrication makes small, lightweight, low power radar sensors feasible for small UAS sense and avoid systems. Long range radar sensors require higher transmit power and consequently become a greater drain on the UAS power budget, or higher antenna directivity, which means a larger antenna size and narrower angular field of view. For this reason, it is important to understand the required sensor detection range for UAS collision avoidance systems.

The minimum required sensing range arises from the time required for SAA operations. The detection and collision avoidance of an imminent threat must be done at a range that is sufficient to allow the SAA system to initiate a track of the detected intruder, detect a collision, plan an avoidance path, and to actually execute the maneuver with sufficient time that result in the minimum required safe distance to the intruder. The current manned aviation regulations has no explicit values for the safe distance, however it is generally understood that the minimum safe distance is required to be at least 500 ft to 0.5 nautical mile in all directions.[2,4] Since the potential ownship and intruder aircraft cover a wide range of vehicle sizes, airframes, weights, designs, etc, the choice of a fixed volume is a substitute for the actual dimensions of the intruder. As shown in Figure 1, the collision volume or the protection zone is a virtual fixed volume boundary centered around the ownship. The general choice for this volume is a cylinder of radius d_s and height h_s centered at the current location of the ownship. A common requirement is a *hockey-puck* collision volume that includes a horizontal distance of 500 ft and a vertical range of 200 ft.[11–13] Then, a collision is defined as an incident that occurs when two aircraft pass less than 500 ft horizontally and 100 ft vertically.

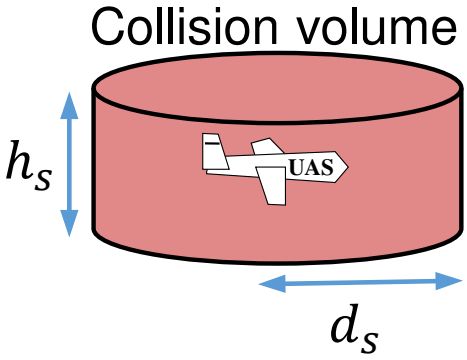

Figure 1. Collision volume and collision avoidance threshold definitions.

In this paper, we present a close form analytical solution to determine the minimum sensing range required for the SAA system to safely avoid an imminent collision. The framework is based on worst-case head-on and overtaking encounter scenarios for aircraft flying roughly at the same altitude. We also discuss an airborne radar sensor that is under development in our group. Its capabilities and limitations, and the feasibility of using it under the assumption of the minimum sensing range required for UAS sense and avoid system is described.

II. Minimum Sensing Range

The minimum required sensing range arises from the time required for SAA operations. The minimum time for the SAA system to be able to track the intruder, detect a collision, plan an avoidance maneuver, and actually fly the maneuver determines the distance at which the UAS must detect the intruder. In other words, the detection of a collision threat must be accomplished at a minimum range allowing the ownship to execute the maneuver with sufficient time that results in the minimum required safe distance from the intruder. A time sequence for the SAA system, similar to that proposed sequence in Ref. 6, is shown in Figure 2. According to the time sequence shown in Figure 2.

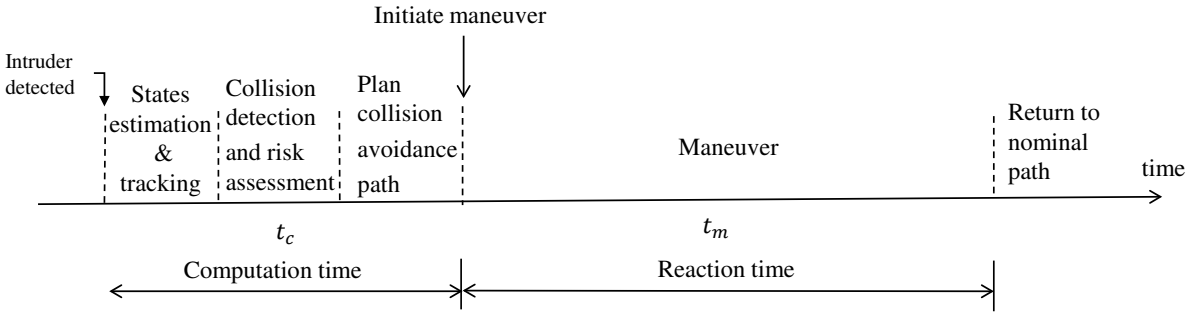

Figure 2. Proposed time sequence of the sense and avoid system.

To compute the sensing range, we first assume an approaching head-on collision encounter scenario similar to the 2D encounter geometry depicted in Figure 3(a). In this encounter scenario the intruder is approaching the ownship in a perfect head-on collision. We also assume that the intruder maintains its direction and speed the entire time of the encounter and that it does not maneuver. Such a situation may exist when encountering a non-cooperative intruder. As shown in Figure 3(a), the required sensing distance can be expressed as

$$d_{\mathrm{r}} = v_c t_c + d_m, \tag{1}$$

where $v_c = v_o + v_i$ is the closing speed, t_c is the computation time required by the SAA system algorithms to track the intruder, detect a collision, plan an avoidance maneuver, and v_o and v_i are the speed of the ownship and the intruder, respectively. From Figure 3(a), d_m can be expressed as $d_m = d_O + d_I$, where $d_O = \sqrt{d_s^2 + 2d_s R_{min}}$, and d_I is the distance traveled by the intruder from the time instant the ownship initiated the maneuver until the time to CPA. d_I can be expressed as $d_I = \frac{v_i}{v_o}\theta R_{min}$, where we have used the fact that the length of avoidance path traversed by the ownship must equal the distance traveled by the intruder to reach the CPA. In other words, $t_{cpa} = \frac{d_I}{v_i} = \frac{L}{v_o}$, where t_{cpa} is the time to closest point of approach, L is the length of ownship's avoidance path, and R_{min} is the minimum turning radius of the ownship. Solving for the d_m gives

$$d_m = \sqrt{d_s^2 + 2d_s R_{min}} + \frac{v_i}{v_o}\theta R_{min}. \tag{2}$$

Then, substituting Eq. (2) in Eq. (1) gives the minimum required sensing range

$$d_{\mathrm{r}}^{(h)} = v_c t_c + \sqrt{d_s^2 + 2d_s R_{min}} + \frac{v_i}{v_o}\theta R_{min}, \tag{3}$$

where the superscript (h) indicates the assumption of the head-on collision encounter scenario. Using θ and R_{min} we can express $d_{\mathrm{r}}^{(h)}$ in terms of known parameters d_s, t_c, v_o, v_i, and maximum banking angle of the ownship. We use the relationship[14]

$$R_{min} = \frac{v_o}{\dot{\psi}_{max}} = \frac{v_o^2}{g\tan\phi_{max}}, \tag{4}$$

where $\dot{\psi}_{max}$ is the heading rate, ϕ_{max} is the maximum banking angle, and g is the gravitational constant. Then, the required sensing range becomes

$$d_{\mathrm{r}}^{(h)} \approx v_c t_c + \sqrt{d_s^2 + 2d_s \frac{v_o^2}{g\tan(\phi_{max})}} + \frac{v_i v_o}{g\tan(\phi_{max})}\arccos\left(\frac{v_o^2}{v_o^2 d_s + g\tan(\phi_{max})}\right). \tag{5}$$

The approximation in Eq. (5) due to the fact that the value of θ is under approximated by the relationship $\theta \approx \frac{R_{min}}{R_{min}+d_s}$. Eq. (5) shows that the closing airspeed of the encountering aircraft, and the maximum banking angle of the ownship affect the required sensing range. In addition, the allowed minimum safe distance that the ownship is required to maintain to the intruder, and the computation time also have an equal contribution in the required sensing range equation.

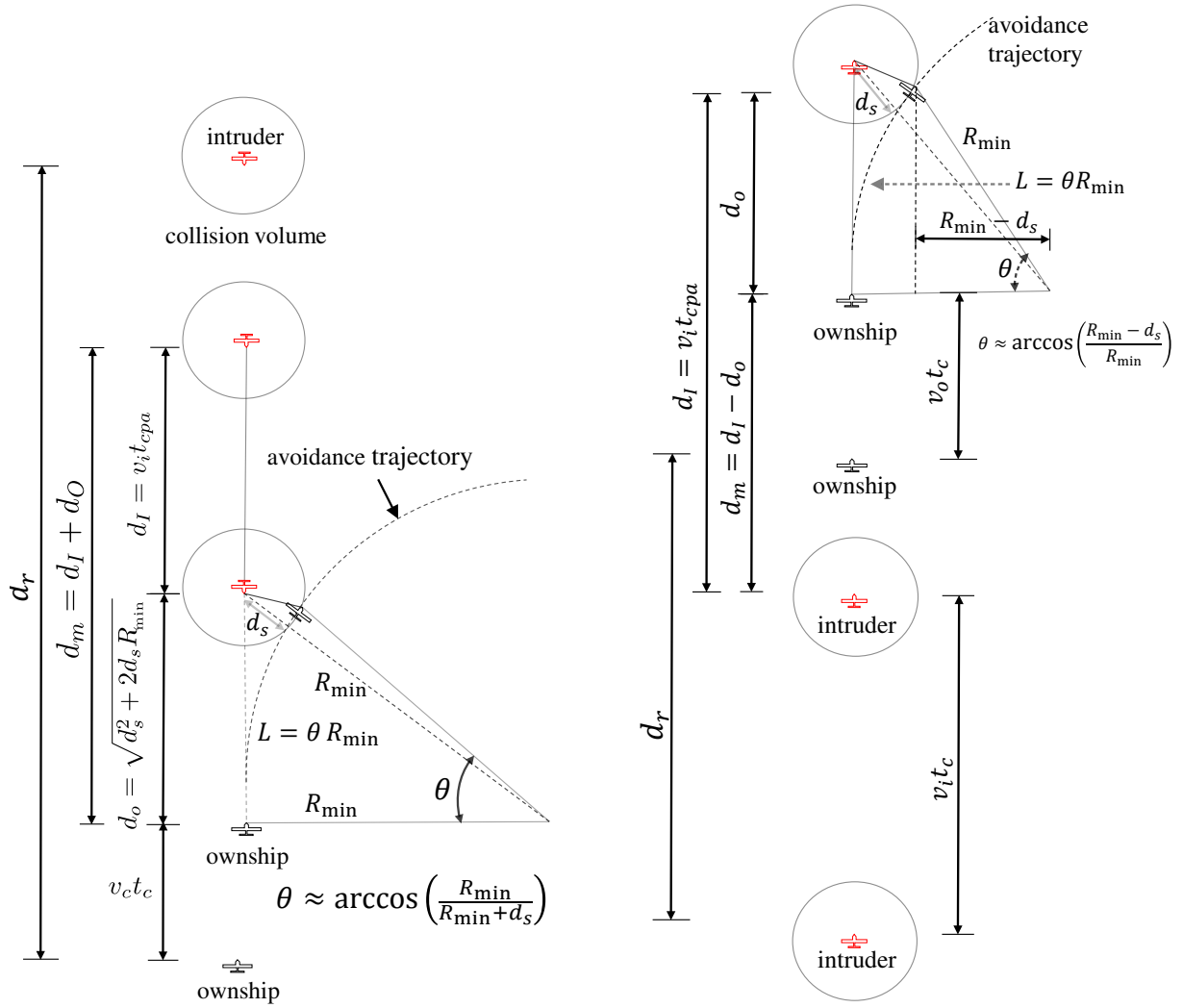

(a) The geometry associated with approaching head-on scenario to estimate the minimum sensing range.

(b) The geometry associated with overtaking scenario to estimate the minimum sensing range.

Figure 3. Encounter geometry to estimate the minimum sensing range.

Another important collision scenario an aircraft may encounter in the airspace is the overtaking collision scenario. The overtaking geometry is shown in Figure 3(b). Similar to the head-on collision scenario discussed earlier in this paper, we assume that the ownship and the intruder are on a perfect collision course, and the intruder does not alter course but maintains its direction and speed during the time of the encounter. Although in manned aviation the overtaken aircraft has the right-of-way as stated in the Code of Federal Regulations (CFR) title 14, (14CFR,§91.113(f)), in the following analysis we will assume a worst-case scenario in which the overtaking aircraft does not alter course possibly because the pilot does not see the UAS. Such situations may exist when operating under visual flight rules where a transponder or a states-reporting device is not required. For instance, a general aviation aircraft flying in G-class airspace at a speed of 100 m/s encounters a slower speed small UAS such as the Raven that has a wingspan of 4.5 ft and flies at a maximum airspeed of 22 m/s. This analysis also implies that the UAS has the sensing capability to detect an overtaking aircraft. Under this assumption, and in similar situations, it is more convenient, and possibly

safer for the smaller UAS to alter course and give the right-of-way to a larger and faster aircraft.

As shown in Figure 3(b), the ownship is required to execute a maneuver that results in a minimum safe distance to the intruder by the time both aircraft reach the closest point of approach. In other words, the length of the avoidance path $L = v_o t_{cpa}$ should equal the distance traversed by the intruder $d_I = v_i t_{cpa}$. Then, solving for d_I gives

$$d_I = \frac{v_i}{v_o} L, \tag{6}$$

where $L = \theta R_{min}$. From the geometry shown in Figure 3(b), d_O can be expressed as $d_O = \sqrt{R_{min}^2 + (R_{min} - d_s)^2}$, then solving for d_m gives

$$d_m = d_I - d_O = \frac{v_i}{v_o}\theta R_{min} - \sqrt{2 d_s R_{min} - d_s^2}. \tag{7}$$

Note that, Eq. (7) is only valid for $R_{min} \geq \frac{d_s}{2}$. However, if $R_{min} = d_s$ then $d_O = d_s$, and $\theta = \arccos(\frac{R_{min} - d_s}{R_{min}})$ equals to 90 deg as shown in Figure 4. And, if $R_{min} = \frac{d_s}{2}$ then θ equals 180 deg as shown in Figure 4. That means the ownship is required to execute a circular arc path that defines a semi-circle of radius R_{min} to result in the minimum safe distance required by the ownship to maintain to the intruder at the closest point of approach. Additionally, when $R_{min} = \frac{d_s}{2}$, d_O equals zero which is an unreasonable solution. Therefore, in this case d_O must be defined to equal d_s. However, in practice when $R_{min} = \frac{d_s}{2}$ the ownship should execute a circular arc followed by a straight line path as shown in Figure 4. In addition, $R_{min} < \frac{d_s}{2}$ suggests that the ownship is too slow to avoid an overtaking scenario. Possible solutions to that are either to increase the ownship speed or to reduce the minimum required safe distance.

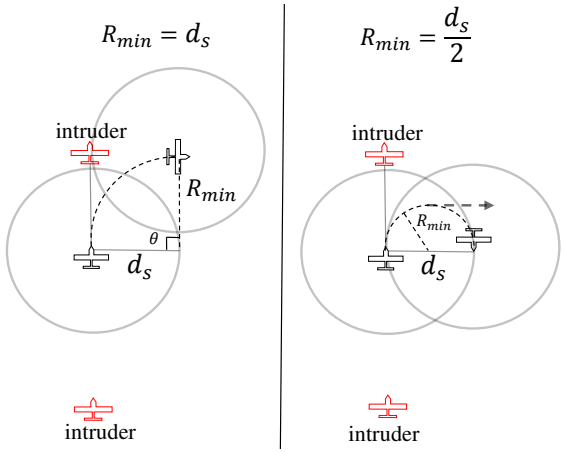

Figure 4. Overtaking scenario, $R_{min} = d_s$, and $R_{min} = \frac{d_s}{2}$.

From the geometry depicted in Figure 3(b), the sensing range is then given by

$$\begin{aligned} d_{\mathrm{r}}^{(o)} &= v_i t_c + d_m - v_o t_c, \\ &= v_c t_c + \frac{v_i}{v_o}\theta R_{min} - \sqrt{2 d_s R_{\min} - d_s^2}, \end{aligned} \tag{8}$$

where the superscript (o) indicates an overtaking collision scenario, and $\bar{v}_c$ is the closing speed defined as $\bar{v}_c = v_i - v_o$. Using the minimum turning radius relationship in Eq. (4) and $\theta \approx \frac{R_{min} - d_s}{R_{min}}$, the minimum required sensing range for an overtaking scenario becomes

$$d_{\mathrm{r}}^{(o)} \approx v_c t_c + \frac{v_i}{v_o} g \tan(\phi_{max}) \arccos\left(\frac{v_o^2}{v_o^2 d_s + g \tan(\phi_{max})}\right) - \sqrt{2 d_s \left(\frac{v_o^2}{g \tan(\phi_{max})}\right) - d_s^2}. \tag{9}$$

Since $d_r^{(h)} > d_r^{(o)}$ because the closing speed in the head-on scenario is always larger than the closing speed in the overtaking scenario i.e. $v_c > \bar{v}_c$, then we have $d_{r_{min}} = d_r^{(h)}$ denote the minimum required sensing range given that the ownship avoids a collision by initiating a turn maneuver. We still, however, need to

know the minimum required sensing range for the overtaking scenario in the case when the ownship uses a separate sensor for rear looking. Since Eqs 5 and 9 under approximate the minimum required sensing range, compensation can be made by selecting a non zero design parameter $\delta_r > 0$ such that the minimum required sensing range becomes

$$\bar{d}_{r_{min}} = (1 + \delta_r) d_{r_{min}}. \tag{10}$$

III. Radar Sensor

The proposed radar sensor is an integrated system comprised of a radio frequency transceiver, analog to digital converters, and signal processing. The radar operates in frequency modulated continuous wave (FMCW) mode, which allows it to operate on much less power than traditional pulsed radar systems. The major system specifications are listed in Table 1. The processing is accomplished using a microZed processor board that features an on-board field programmable gate array (FPGA) in addition to the central processing unit (CPU). The FPGA executes the computationally intense radar processing, while the operations of collision risk assessment and avoidance path planning are performed on the CPU, which communicates way-points to an external autopilot unit.

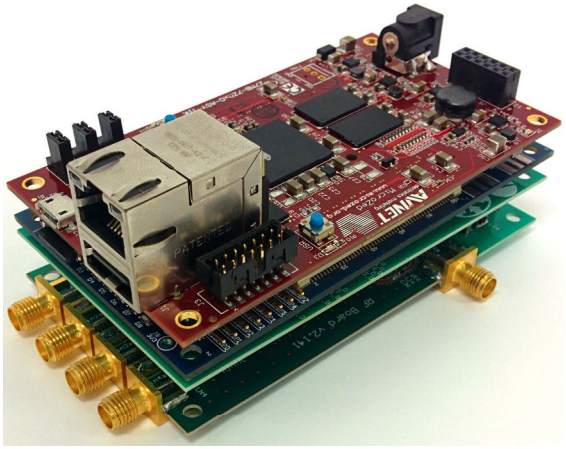

Figure 5. Portable radar system designed for use on-board UAS.

Objects are only visible to the naked eye if they can reflect visible light. In a similar manner, objects are only visible to a radar if they can reflect radio waves at the frequency of operation. This ability to reflect radio waves is called the radar cross section (RCS) of the object and arises from the material and geometric properties of the target. The ability to detect an intruder depends as much on the properties of the radar system, such as transmitted power and antenna gain, as it does on the properties of the intruder. The direct dependence on the system properties and intruder properties is evident in the standard radar equation for received power P_{rec} given by

$$P_{rec} = \frac{P_{trans} G^2 \sigma_{\text{RCS}} \lambda^2}{(4\pi)^3 r^4}, \tag{11}$$

where P_{trans} is the transmitted power, G is the gain of both the transmitter and receiver respectively, σ_{RCS} is the radar cross section of the target, λ is the wavelength and r is the range to the target.[15] RCS is a strong function of both the frequency of operation and the angle of observation to the target. However when the size of the target is much larger than the wavelength of operation, the calculation can be simplified using geometrical approximations. Although RCS data is not available for every type of aircraft, the data that is available correlates quite closely with geometrical approximations for those aircraft. This correlation justifies the use of geometrical approximations for rough RCS estimates when published data is not available, and is therefore the approach taken in this paper.

The radar system shown in Fig. 5 was able to detect human targets with an RCS of 1 m^2 at a range of 150 m using antennas with a gain of 13 dB each. The range at which the radar system can observe a target can be increased by transmitting more power or by using antennas with a higher gain. This relationship is evident in Eq. (11), however both options have trade-offs. Transmitting more power will always extend the

Table 1. Radar Sensor Parameters

Parameter	Value	Parameter	Value
Size	2.25in x 4in x 1in	Weight	120 g (0.26 lbs)
Consumed Power	8 watts	Approx. Cost of Materials	US$1000
Transmitted Power (P^{trans})	5 miliwatts	Center Frequency	10.25 GHz
Chirp Period (T_c)	1 ms	Chirp Bandwidth	500 MHz
System Noise Figure (F)	8 dB	ADC sample rate	1 Msamp/s

range of a radar system, but there are both legal and practical limits to the amount of transmitted power. At 10 GHz, where this system operates, the legal transmission limit in the USA is 5 watts of radiated power. Even though this is considerably lower than what many military radars transmit, it still imposes practical limitations for operation on UAS. Power amplifiers generally have a power added efficiency of approximately 20%, so in order to transmit 5 watts of power, the system would require at least 25 watts of battery power, which would severely limit the flight time of smaller aircraft.

Manipulating the antenna configuration of a radar system can also provide the needed gain to detect far away targets, but this also comes at a cost. Higher gain antennas have, by definition, smaller beamwidths and are larger in size. When a set of low gain antennas are used, their beams cover a broad field of view. This can be quite advantageous in a phased array antenna configuration where the total field of view is dictated by the pattern of a single element. A phased array system requires no mechanical scanning and can track multiple targets simultaneously. In situations where higher gain antennas are needed, phased array systems are still used, however, the scanning area is restricted. When both high gain and high angular resolution are needed, the traditional method is to place the high gain antenna on a mechanical gimbal. A final option is the combination of a phased array system with a mechanical gimbal. This configuration offers the user high angular resolution and could provide a field of view of a full 360 deg in both elevation and azimuth. In applications involving large aircraft, the user could place one radar system at the nose of the aircraft and one radar system at the tail of the aircraft in order to achieve full coverage. In the following section we provide a brief practical analysis of the transmitted power and antenna configurations required for each of the UAS listed in Table 2 to detect an intruder with sufficient time to avoid collision.

IV. Simulation Results

The analysis results shown in Table 2 illustrate the validity of the geometry-based analytical solution presented in Section II to design the minimum required sensing range for a sense and avoid system. We consider Eqs. (5), and (9) for the worst-case horizontal head-on and overtaking collision scenarios, respectively. We have assumed that the computation time t_c is 5 s, and the performance characteristics of aircraft are given in Table 2.

Table 2. Sensing range required for SAA system. The symbols H and O are abbreviations for head-on and overtaking collision scenarios, respectively. The numerals marked with asterisk are our best estimate.

Intruder			Raven RQ-11B		ScanEagle		Altus II		Cessna SkyHawk		Airtractor AT-802F	
Ownship			Sensing range (m)									
	v m/s	$\psi_{\max}$ deg.	H	O	H	O	H	O	H	O	H	O
Raven RQ-11B	22	30*	545	–	729	435	825	581	961	786	1,290	1,282
ScanEagle	41	30*	787	–	999	–	1,111	183	1,267	361	1,646	792
Altus II	51	30*	912	–	1,130	–	1,245	–	1,406	219	1,797	646
Cessna SkyHawk	65	–										
Air Tractor AT-802F	99	–										

It is an obvious conclusion from these results, that a SAA-equipped UAS will require a sensor to provide higher sensing range with increasing speed of encountering aircraft. For instance, if the Raven RQ-11B is

required to fly in a specific portion of the airspace in which it expects to encounter a similar type of Raven, ScanEagle and Altus II, then the Raven is required to be equipped with a sensor that is capable of providing a minimum sensing range of 825 m. If a slack parameter of $\delta_r = 0.25$ is used, then the required sensing range becomes $\bar{d}_{r_{min}} = 1.031$ km. However, if any of the aircraft shown in Table 2 might be encountered, then a sensor with a minimum range of 1.29 km is required. If a slack parameter of $\delta_r = 0.25$ is used, then the required sensing range becomes $\bar{d}_{r_{min}} = 1.613$ km. To demonstrate the validation of the minimum required sensing computed in Table 2. We simulate a simple case scenario similar to the encounter geometry shown in Figure 6. The ownship with dynamic characteristics similar to Raven RQ-11B starts at position (0,0) with initial heading of 0 degrees to the y-axis and moving with constant speed of 22 m/s. The intruder starts at position (0, 1613) with 180 degrees with respect to the y-axis and moving at speed of 99 m/s. The ownship keeps moving on the same path for 5 s which is the time we have assumed that it needs to track, detect a collision and plan for it, and then it turn maneuver followed by a a straight path to avoid the collision as shown in Figure 6(a). Figure 6(b) shows that the ownship avoids the intruder and maintains the required minimum safe distance d_s to the intruder given that it detected the intruder at 1.613 km.

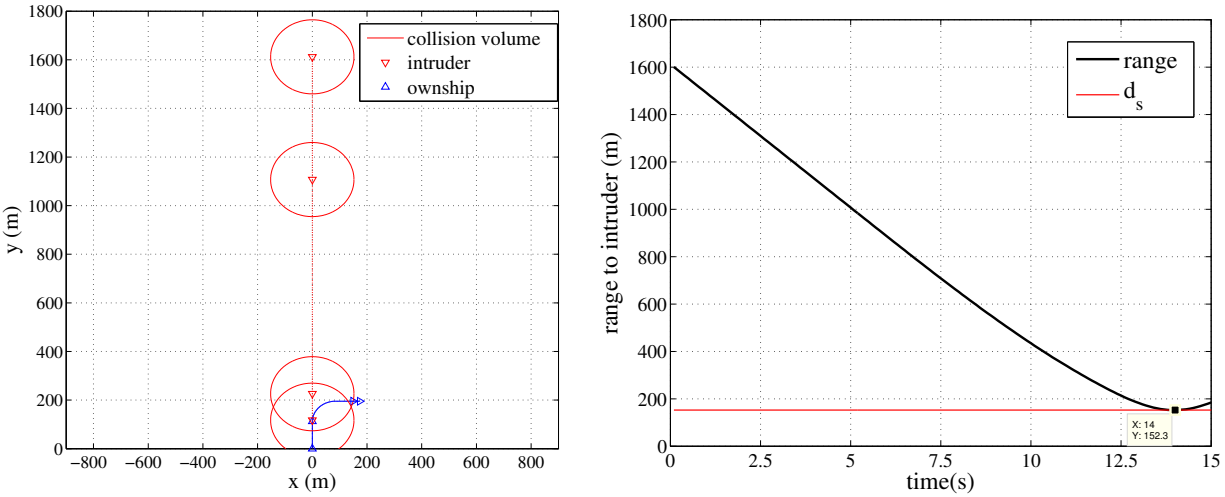

(a) Overhead view of SAA operation based on minimum sensing range of $\bar{d}_{r_{min}} = 1.613$ km.

(b) Range between ownship and intruder.

Figure 6. Simulation results using ownship dynamic model similar to Raven RQ-11B and intruder similar to Airtractor AT-802F.

The data in Table 2 can also be used to analyze the requirements on the sensor as well, however the dependence of the sensor on RCS adds another dimension to consider. The specifications listed in Section III and Eq. (11) predict that in order for this radar system to detect a target, it must receive at least 1.7 pico-watts of power. Using the RCS of each aircraft, we solve Eq. (11) for the antenna gain necessary for each aircraft to detect an intruder at the defined sensing range. If the calculated values for required antenna gain fall within a realistic range, we can conclude that the system is feasible. We assume that the ScanEagle and Altus II operate at the maximum transmittable power level of 5 watts because their payloads are large enough to store the necessary batteries. In like manner, we assume the Raven transmits only 0.4 watts of power, in an effort to maintain low power requirements and not limit flight time. The results are shown in Table 3.

From these results it is evident that detecting the aircraft with small RCS is far more difficult than detecting the larger aircraft, despite the fact that they require a much smaller sensing range. The larger payload sizes of the Altus and the ScanEagle would make it easier to implement an antenna system, gimbaled or otherwise, that would permit the safe detection of other aircraft. On the other hand, the Raven has an extremely small payload capacity, and the required values of gain are reasonable enough that a phased array system could successfully be implemented on the Raven if aerodynamic antennas were used that could be attached to the wings. For a four channel phased array system such as the one described in this paper, the resulting field of view for the gain specified would be approximately 90 deg by 15 deg.

Table 3. Antenna gain requirements for detecting intruders of specified RCS. An asterisk marks intruders for which geometrical approximations were used to estimate RCS. All other values were found courtesy of Ref. 16

Intruder				Raven RQ-11B	ScanEagle	Altus II	Cessna SkyHawk	Airtractor AT-802F
Ownship	RCS m^2	Payload kg	P_{trans} watt	Required Antenna Gain (unitless)				
Raven RQ-11B	0.032*	0.36	0.4	166	167	68	52	53
ScanEagle	0.1	6	5	99	89	35	25.5	24
Altus II	1*	150	5	132	114	44	31.5	29
Cessna SkyHawk	3.16	-	-					
Air Tractor AT-802F	10*	-	-					

V. Conclusions and Future Work

The potential to integrate UAS into the national airspace is highly dependent on their ability to sense and avoid other air traffic. Based on a worst-case collision encounter geometry, the minimum sensing distance required to safely execute a collision avoidance maneuver was calculated. This minimum sensing distance took into account the computation time involved in target tracking, risk assessment, and path planning in addition to the actual reaction time required to execute the collision avoidance maneuver. The results listed in Table 2 demonstrate the need for a sensor with a moderate sensing range of 1 to 2 kilometers and high range accuracy.

Radar was selected as the primary sensor because it offers the best performance in non-cooperative scenarios where high range resolution is needed. An analysis was performed to determine whether this could be accomplished on-board small UAS, similar to a Raven RQ-11B. A portable radar sensor under development was used as a benchmark to judge its feasibility for SAA. Our analysis determined that the antenna properties required to detect intruders at a safe distance were quite reasonable, especially for the larger UAS. Although the system appeared feasible for a UAS similar to the Raven, the implementation of a radar system on any aircraft with a smaller payload than the Raven would be impractical. It was found that the antenna requirements are affected more by RCS than they are by range. Any radar-based SAA system designed to detect small RCS intruders at a close range will be powerful enough to detect large RCS intruders from far away.

This work can be expanded to include collision encounter geometry in 3D. Future work also includes implementing the derived antenna parameters to determine whether they actually meet the minimum required sensing ranges. We are currently working towards implementing a radar-based SAA system using the phased array radar prototype discussed in this paper applying lessons learned from this work.

Acknowledgment

This research was conducted in the Center for Unmanned Aircraft Systems (C-UAS) with support from the National Science Foundation I/UCRC program grant number IIP-1171036 and C-UAS Industry Advisory Board members.

References

[1]Contarino, M. and Scire Consultants, L., "All Weather Sense and Avoid System for UASs," Tech. rep., Report to the Office of Naval Research, 2009.

[2]"Standard Specification for Design and Performance of an Airborne Sense-and-Avoid System," 2007.

[3]Dalamagkidis, K., Valavanis, K. P., and Piegl, L. A., *On Integrating Unmanned Aircraft Systems into the National Airspace System*, Vol. 52, Springer Science+Business Media B.V., 2nd ed., 2012.

[4]Angelov, P., *Sense and Avoid in UAS: Research and applications*, John Wiley & Sons, Ltd., 2012.

[5]Prats, X., Delgado, L., Jorge, R., Pablo, R., and Pastor., E., "Requirements, Issues, and Challenges for Sense and Avoid in Unmanned Aircraft Systems," *Aircraft*, Vol. 49, No. 3, 2012, pp. 677–687.

[6]Geyer, C., Singh, S., and Chamberlain, L., "Avoiding Collisions Between Aircraft: State of the Art and Requirements for UAVs operating in Civilian Airspace," Tech. rep., Jan 2008.

[7]Boskovic, J. D., Jackson, J. A., and Mehra, R. k., "Sensor and Tracker Requirements Development for Sense and Avoid Systems for Unmanned Aerial Vehicles," *AIAA Modeling and Simulation Technologies (MST) Conference*, Boston, MA, Sep 2013.

[8]Melnyk, R., Daniel, S., Vitali, V., and Hernando, J., "Sense and Avoid Requirements for Unmanned Aircraft Systems Using a Target Level of Safety Approach," *Risk Analysis*, Vol. 34, No. 10, 2014, pp. 1894–1906.

[9]Sahawneh, L. R., Mackie, J., Spencer, J., Beard, R. W., and Warnick, K. F., "Airborne Radar-Based Collision Detection and Risk Estimation for Small Unmanned Aircraft Systems," *Aerospace Information Systems*, Vol. 0, No. 0, 2015, pp. Ahead of Print: 1–11.

[10]R. H. Chen A.Gevorkian, A. F. and Chen, W.-Z., "Multi-Sensor Data Integration for Autonomous Sense and Avoid," *American Institute of Aeronautics and Astronautics (AIAA)*, 2011.

[11]Lee, S. M., Park, C., Johnson, M. A., and Mueller, E. R., "Investigating Effects of ï£ · Well Clearï£ · Definitions on UAS Sense-And-Avoid Operations," *Aviation Technology, Integration, and Operations Conference*, AIAA, Los Angeles, CA, 2013.

[12]Consiglio, M., Chamberlain, J., Munoz, C., and Hoffler, K., "Concept of Integration For UAS Operations in The NAS," *28th International Congress of the Aeronautical Sciences (ICAS)*, Brisbane, Australia, 2012.

[13]Workshop, F. A. A., "Sense and Avoid (SAA) for Unmanned Aircraft Systems (UAS)," 2009.

[14]Beard, R. and McLain, T., *Small Unmanned Aircraft: Theory and Practice*, Princeton University Press, 1st ed., 2012.

[15]Richards, M. A., Scheer, J., and Holm, W. A., *Principles of Modern Radar: Basic Principles*, SciTech Publishing, Inc., 2010.

[16]Wilson, M., "Ground-Based Sense and Avoid Support for Unmanned Aircraft Systems," *28TH Congress of the International Council of the Aeronautical Sciences*, 2012, pp. 2012–11.3.3.